

Article

Study on Mechanical and Rheological Properties of Solid Waste-Based ECC

Xiao Wang ^{1,2}, Ke Sun ^{3,4}, Jingga Shao ^{2,5} and Juntao Ma ^{3,4,*}

¹ School of Materials Science and Engineering, North China University of Water Resources and Electric Power, Zhengzhou 450045, China

² Green High-Performance Material Application Technology Transportation Industry Research and Development Center, Henan Jiaoyuan Engineering Technology Group Co., Ltd., Zhengzhou 451450, China

³ International Joint Research Lab for Eco-Building Materials and Engineering of Henan, North China University of Water Resources and Electric Power, Zhengzhou 450045, China

⁴ School of Civil Engineering and Communication, North China University of Water Resources and Electric Power, Zhengzhou 450045, China

⁵ Henan College of Transportation, Zhengzhou 451450, China

* Correspondence: majuntao@ncwu.edu.cn

Abstract: As one of the main raw materials of engineered cementitious composite (ECC), fly ash exerts the “ball effect” and “pozzolanic effect” in concrete, which improves the working performance of concrete and enhances the strength of the concrete matrix. Polyvinyl alcohol (PVA) fiber has been widely used in the preparation of ECC, while ground fly ash can be used to enhance the performance of ECC as a kind of high-activity admixture. In this paper, the compressive strength, flexural strength and flexural toughness of ECC prepared from different types of fly ash (raw fly ash, sorted fly ash and ground fly ash) are compared, and the rheological properties of the ECC are analyzed by studying the two parameters of yield stress and plastic viscosity. The results show that the smaller the particle size of fly ash is, the more sufficient it reacts with Ca(OH)₂ produced by cement hydration, and the more it can improve the compressive strength and flexural strength of the matrix. In addition, the smaller the particle size of fly ash, the higher the yield stress and plastic viscosity of ECC; therefore, the distribution of PVA fiber in ECC is more uniform, thereby improving the flexural toughness and ductility of ECC.

Keywords: engineered cementitious composite; PVA fiber; ground fly ash; flexural toughness; rheological properties



Citation: Wang, X.; Sun, K.; Shao, J.; Ma, J. Study on Mechanical and Rheological Properties of Solid Waste-Based ECC. *Buildings* **2022**, *12*, 1690. <https://doi.org/10.3390/buildings12101690>

Academic Editors: Huazhe Jiao, Juanhong Liu, Lei V. Zhang and Xiaoyong Wang

Received: 7 September 2022

Accepted: 10 October 2022

Published: 14 October 2022

Publisher's Note: MDPI stays neutral with regard to jurisdictional claims in published maps and institutional affiliations.



Copyright: © 2022 by the authors. Licensee MDPI, Basel, Switzerland. This article is an open access article distributed under the terms and conditions of the Creative Commons Attribution (CC BY) license (<https://creativecommons.org/licenses/by/4.0/>).

1. Introduction

Cement-based composite materials have been the most widely used building materials since the 19th Century, due to their advantages of abundant raw materials, low production cost, high strength, good adaptability and convenient construction [1]. However, due to the shortcomings of high brittleness and low strain of cement-based composites, brittle cracks and failure will occur when the ultimate load is reached, which limits the application of cement-based composites [2]. Therefore, it is very important to develop cement-based composites with high ductility.

Some scholars have improved the toughness and ductility of the matrix by adding fibers. Marcalikova studied the influence of different types and quantities of steel fibers on the ductility of the matrix [3]. The results show that tensile strength and fracture energy increase with the increase of steel fiber content. Steel fibers can significantly enhance the strength of concrete and effectively reduce the occurrence of large cracks, but the improvement effect on small cracks is not good. Pujadas [4] studied the cracking problem of concrete by adding plastic fibers. It found that the fracture mechanical properties of plastic fiber concrete were not fundamentally different from ordinary concrete, and the brittle failure and cracking problems of concrete could not be solved.

In 1990, Professor Victor Li [5] from the University of Michigan, USA, based on the theories of micromechanics and fracture mechanics, optimized the performance and relationship between fiber, cement-based material and interface transition zones, and designed a new engineered cementitious composite (ECC) with pseudo strain-hardening characteristics and multi-crack-cracking characteristics [6]. When ECC is damaged by bending, it experiences elastic stage, yield stage, strengthening stage and failure stage. In the strengthening stage, when the stress exceeds the cracking strength, the stress-strain curve does not decrease but fluctuates. In this process, ECC continuously absorbs energy and produces many tiny cracks. The tensile strain of ECC is 2~5%, which is hundreds of times that of ordinary concrete, so it is widely used in repairing structures, seismic structures, long-span structures and other structures [7].

Haskett [8] studied the compressive zone and tensile zone of ECC beams, and found that PVA fiber in the compressive zone effectively restrained the cracking of concrete, slowed down the damage of the internal structure and transferred tensile stress in the tensile zone. Therefore, PVA fiber concrete has good ductility and good performance after cracking. In order to study the influence of fiber on the bending properties of concrete. Li [9] studied the influence of different fiber content on the flexural properties of concrete by conducting three-point bending tests on notched beams. The results show that the addition of fibers can improve the peak strength and fracture energy of the matrix, and reduce the crack growth rate and initial crack width. Through a PVA fiber pull-out test and a bending test, Niu [10] studied the influence of PVA fiber matrix interface properties on ECC performance. The results show that the ECC with good ductility cannot be obtained by directly adding PVA fiber, and that the interface property between fiber and the matrix determines the effect of PVA fiber. In recent years, some studies have shown that the addition of fly ash [11–15] can improve the mechanical properties of cementitious materials, and can also be used to improve the mechanical properties of ECC. In general, ordinary cement-based composites use 10–25% fly ash instead of cement, and engineering cement-based composites use approximately 40–60% fly ash, thus achieving superior environmental performance [16].

Research by Zhang [17] shows that the addition of fly ash improves the later hydrate age compressive strength of ECC. With the increase in temperature, the high content fly ash group showed good strain-hardening characteristics, while the low content fly ash group showed obvious deterioration in tensile properties. Jamal Khatib [18] used different amounts of fly ash instead of cement to study its effect on the strength of ECC beams. The results show that 20% fly ash has the highest compressive strength, tensile strength and elastic modulus. The three-point bending test shows that the beam with 20% fly ash has the best bearing capacity and ductility.

Adding a certain amount of fly ash into ECC can improve its mechanical properties. However, some scholars [19] have studied that when the addition of fly ash in self-compacting concrete is too high, there are less CSH cementitious materials generated by cement hydration reaction, and a large number of unreacted fly ash particles remain in the matrix, leading to the reduction of matrix strength and resulting in a low utilization rate of fly ash. In order to improve the utilization of fly ash, the activity of fly ash can be improved by reducing the particle size of fly ash after separation or mechanical grinding. Ma [20] and Chen [21] found that, compared with the original fly ash, the finely ground fly ash was more likely to exert the pozzolanic effect and higher strength. However, due to the change in morphology, ground fly ash will affect the dispersion of PVA fibers in the matrix, which will enhance the strength of the matrix and affect the working performance of concrete.

In summary, most scholars have studied the influence of fly ash content on ECC performance without considering the influence of fly ash type on ECC. Therefore, based on the preparation of PVA fiber ECC, finely ground fly ash, undisturbed fly ash and separated fly ash were added in this paper. The effects of different types of fly ash on the mechanical

and rheological properties of concrete were studied, and the mechanism of different types of fly ash on the mechanical and rheological properties of ECC was also revealed.

2. Materials and Methods

2.1. Materials

The fly ash used in the test came from the Yanshi China Resources Power Plant; chemical composition is shown in Table 1. In order to analyze the effect of fly ash with different types, the fly ash was sorted and milled. The sorting process used pneumatic sorting to obtain fly ash that meets the requirements of Class I fly ash, and the grinding process used a laboratory SM–500 ball mill for 30 min to obtain ground fly ash. The size distribution curves (see Figure 1) and SEM images (see Figure 2) of the raw fly ash, the sorted fly ash and the ground fly ash were compared experimentally, and their performance parameters are shown in Table 1.

Table 1. Chemical composition of cement and fly ash (wt%).

Chemical Composition	CaO	SiO ₂	Al ₂ O ₃	Fe ₂ O ₃	MgO	SO ₃	Others
Cement	61.74	16.44	4.78	3.52	2.67	3.69	7.16
Fly ash	3.54	53.72	28.11	11.55	0.78	0.42	1.88

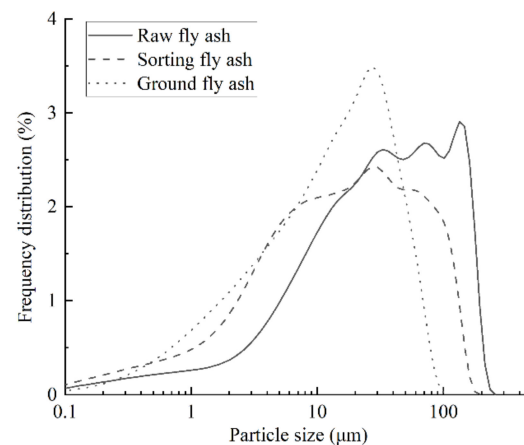


Figure 1. Laser particle size distribution curve of fly ash.

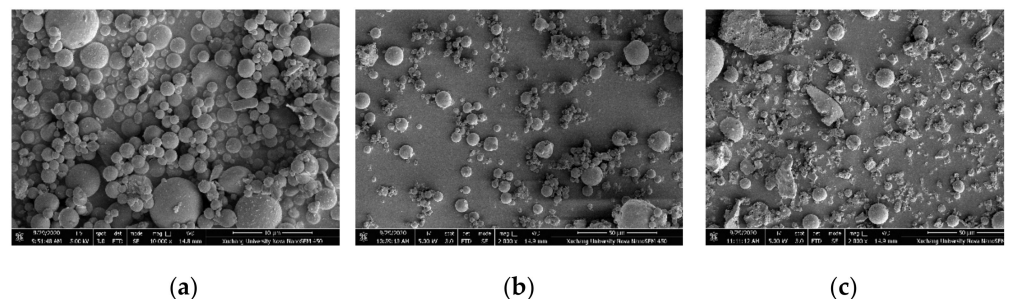


Figure 2. SEM image of fly ash: (a) raw fly ash; (b) sorted fly ash; (c) ground fly ash.

As shown in Figures 1 and 2, the particle size of the raw fly ash was mostly distributed in 1~250 μm , and the shape was mostly spherical particles with a smooth surface. After sorting, the particle size of the fly ash was concentrated between 2 and 200 μm , and the particle morphology was spherical particles with a smaller particle size than that of the raw fly ash. The particle size of the ground fly ash was concentrated between 1 and 90 μm , and because the shell wall of the fly ash was damaged in the grinding process, many irregular

particles and fly ash with a smaller particle size were produced. Therefore, the difference between the three types of fly ash mainly lay in particle size and morphology.

The cement adopted was P·O 42.5 ordinary Portland cement, produced by Henan Tianrui cement factory; the chemical composition is shown in Table 1. The quartz sand apparent density was 2.6 g/cm³. The PVA fiber used was Japanese Kuraray fiber, with an elastic modulus of 43 GPa, a tensile strength of 1469 MPa and an ultimate elongation of 6.3%. The emulsion powder was German Wacker brand, and the apparent density was 450 g/L.

2.2. Specimen Preparation

The test was conducted in accordance with the test method specified in the Chinese National Standard GB/T 17671/2021 “Test Method for Cementitious Sand Strength (ISO Method)”. By mixing different particle sizes of fly ash, mortar test blocks were prepared with the specifications of 40 mm × 40 mm × 160 mm. The water cement ratio was 0.35, the volume admixture of PVA fiber was 2% and the mass admixture of rubber powder was 1.8%; the test proportion is shown in Table 2. The prepared mortar blocks were placed in a standard environment for 3 days and 28 days.

Table 2. Proportional design of ECC/g.

Number	Cement	Raw Fly Ash	Sorted Fly Ash	Ground Fly Ash	Quartz Sand	Emulsion Power	PVA Fiber	Water	Water Reducer
P1	968.4	107.6	0	0	484	26.9	23.96	376.6	5.38
P2	968.4	0	107.6	0	484	26.9	23.96	376.6	5.38
P3	968.4	0	0	107.6	484	26.9	23.96	376.6	5.38

The specimens were prepared as follows: add cement, rubber powder and fly ash into the cement mortar mixer, and slowly stir for 60 s at a speed of 140 r/min. After the mixing is uniform, add water and water reducer and continue mixing for 30s. After adding quartz sand, slowly stir for 30 s, and quickly stir for 60 s at a speed of 280 r/min. After adding PVA fiber, slowly stir for 60 s, and finally quickly stir for 120 s to complete the mixing. The mixture was then poured into a mold, vibrated and cured at room temperature for 24 h. Finally, the mixture was cured in a standard curing room for 28 days.

2.3. Test Device and Methods

2.3.1. Compressive Strength and Flexural Strength Test

The prepared mortar blocks of three fly ash types were maintained for 3 days and 28 days, and then they were tested for compressive strength and flexural strength according to GB/T17671–2021 “Test Method for Cementitious Sand Strength (ISO Method)”.

2.3.2. Bending Toughness Test

The load deflection curve and bending toughness of the mortar blocks of different ages were tested using a UTM–5105 testing machine (produced by JiNan LiHua test system Co., Ltd., see Figure 3) at a loading speed of 0.2 mm/min. The bending test refers to Chinese local standard DBJ61/T 112–2021 technical specification for application of ECC, and the bending toughness test was conducted on mortar blocks after curing for 3 days and 28 days. The bending toughness of the mortar block was calculated with reference to DBJ61/T 112–2021. The calculation formula is as follows:

$$W_u^e = \frac{\Omega_u}{bh^2} \quad (1)$$

where, W_u^e represents the equivalent bending toughness; Ω_u represents the area enclosed by the deflection and curve corresponding to 0.85 times of the peak load; b, h represent the width and height of the block, respectively.

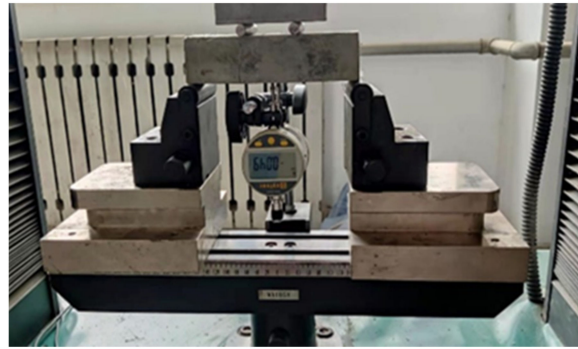


Figure 3. UTM–5105 testing machine.

2.3.3. Rheological Test

The PVA fiber and quartz sand were removed from the original proportion to obtain a fly ash slurry, and the rheological properties were tested using an RST–SST rheometer (see Figure 4) produced by Brookfield, Massachusetts, USA, to analyze the effect of the different types of fly ash on the matrix properties [22]. The yield stress and plastic viscosity are calculated as follows:

$$\tau = \tau_0 + \mu\gamma \quad (2)$$

where, τ represents the shear stress; τ_0 represents the yield stress; μ represents the plastic viscosity; γ represents the shear rate.



Figure 4. RST–SST rheometer.

3. Result and Discussion

3.1. Effect of Different Types of Fly Ash on Compressive and Flexural Strength of ECC

The test results are shown in Figure 5. From Figure 5a, it can be seen that the compressive strength of the mortar blocks increases with the decrease in the fly ash particle size. For the 3 days compressive strength, the P3 group improves by 11.4% and 5.8% compared to the P1 and P2 groups, and for the 28 days compressive strength, the P3 group improves by 9.7% and 4.2% compared to the P1 and P2 groups, respectively. The hydration products of cement paste are mainly CSH and Ca(OH)_2 , after the addition of fly ash. Since fly ash is a kind of artificial pozzolanic admixture, its hydration reaction can only be carried out under alkali excitation. The hydration reaction speed of raw fly ash particles is slow, so they basically do not participate in the hydration reaction in the early stage and pores appear around the fly ash particles, which increases the porosity in the ECC paste and decreases the matrix strength. Combining Figures 1 and 2, it can be seen that the particle size of the fly ash after sorting and grinding is significantly reduced, and the fly ash can fully fill the pores in the mortar block and increase its compactness. Therefore, for the 3 days compressive strength $\text{P3} > \text{P2} > \text{P1}$.

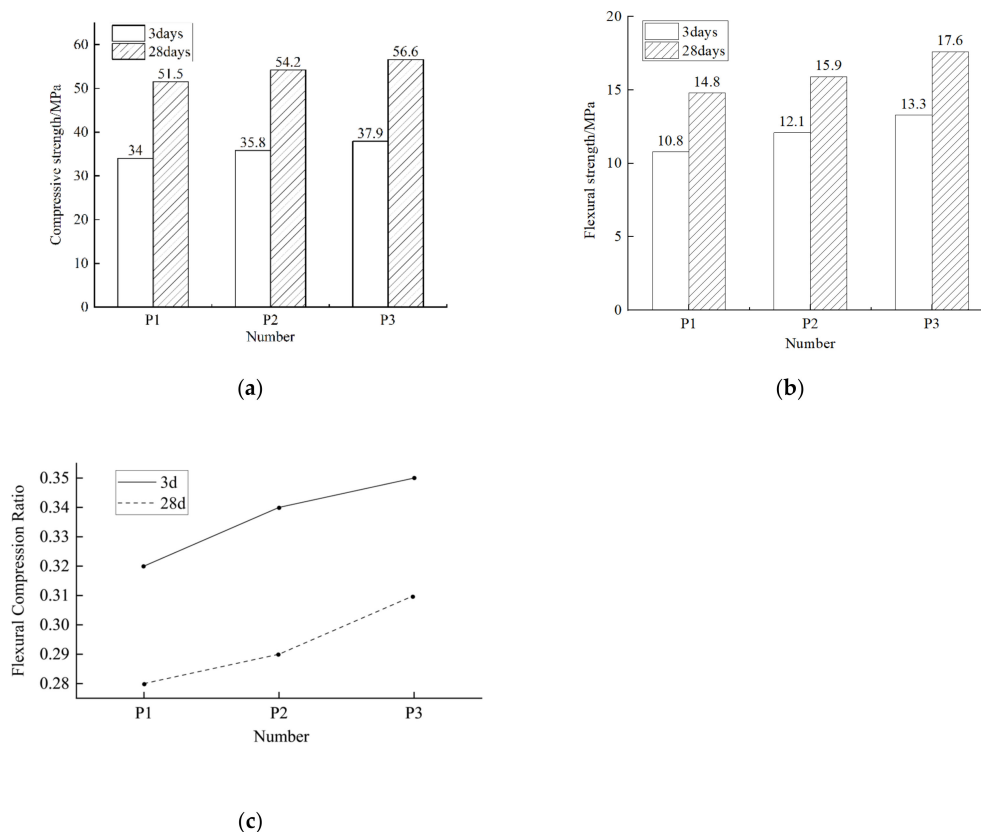


Figure 5. Mechanical property curve of ECC prepared with different types of fly ash: (a) compressive strength; (b) flexural strength; (c) flexural compression ratio.

With the increase of hydration age, SiO_2 , Al_2O_3 and other silicates in fly ash react with $\text{Ca}(\text{OH})_2$ generated by the hydration reaction of cement, occurring as a secondary hydration reaction [23] to produce hydrated calcium silicate, which fills the pores in the matrix and enhances the strength of the matrix. Compared with the raw fly ash, the particle size of the sorted fly ash is reduced, the specific surface area is increased and, when the water–cement ratio is reduced under the condition of maintaining the same water consumption, the fly ash can give rise to the pozzolanic effect and react with $\text{Ca}(\text{OH})_2$. Meanwhile, the particle size is small, and the particles can fill the pores in the slurry well, making the fly ash cement slurry denser. Therefore, the P2 ECC shows a higher compressive strength than that of P1 ECC. The P3 ECC with the ground fly ash shows better mechanical properties because its particle morphology is greatly damaged; the internal active substances are released, and it more easily reacts with $\text{Ca}(\text{OH})_2$ in the cement slurry. Therefore, for the 28 days compressive strength $\text{P3} > \text{P2} > \text{P1}$.

It can be seen in Figure 5b that the flexural strength of the mortar block increases with the decrease in the fly ash particle size. Compared with the P1 and P2 groups, the flexural strength of the P3 group increased by 23.14% and 9.91% at 3 days, and by 18.92% and 10.69% at 28 days, respectively. The flexural compression ratio is one of the indexes used to measure the toughness of concrete; the larger its value, the better the toughness of the concrete. According to Figure 5c, as the particle size of the fly ash decreases, the flexural compression ratio increases, indicating that the smaller the particle size of ground fly ash is, the more conducive it is to the development of mortar block toughness. This is because not only does the ground fly ash give rise to the pozzolanic effect and microaggregate effect, and increase the matrix strength, but it also improves the dispersion uniformity of the PVA fiber in the matrix to a certain extent. When cracks appear in the mortar block, countless PVA fibers randomly distributed on both sides of the crack provide excellent crack resistance and limit the further expansion of cracks. The fibers in group P3 are more

evenly distributed than those in groups P1 and P2, and the proportion of fibers bearing tensile stress increases; thus showing higher flexural strength.

3.2. Effect of Different Types of Fly Ash on Bending Toughness of ECC

Figure 6 shows the load deflection curves of the ECC prepared with different types of fly ash. The ECC prepared with different types of fly ash shows good strain-hardening characteristics [24] under load. As can be seen in Figure 6b, the fracture load of the P3 group at 28 days was 2954 N. Compared with the P1 and P2 groups, the fracture load of P3 group increased by 33.6% and 27.8%, respectively. When cracks appear in the mortar block under load, they do not form complete cracks immediately, but continue to carry and continuously produce microcracks under the anchoring action of the PVA fibers between the cracks. In the strain-hardening stage, the deflection of the P3 group increased the most, reaching 1.577 mm; compared with the P1 and P2 groups, it increased by 60.9% and 51.6%, respectively, indicating that the P3 group has the largest deformation capacity and ductility in this stage. At the same time, the area of the load-deflection curve of the P3 group is the largest, and it shows that the P3 group test block absorbs the most energy and has the strongest toughness during bending failure. Therefore, the P3 group shows better bending toughness and ductility under load. According to the calculation formula (1), the calculation results are shown in Table 3.

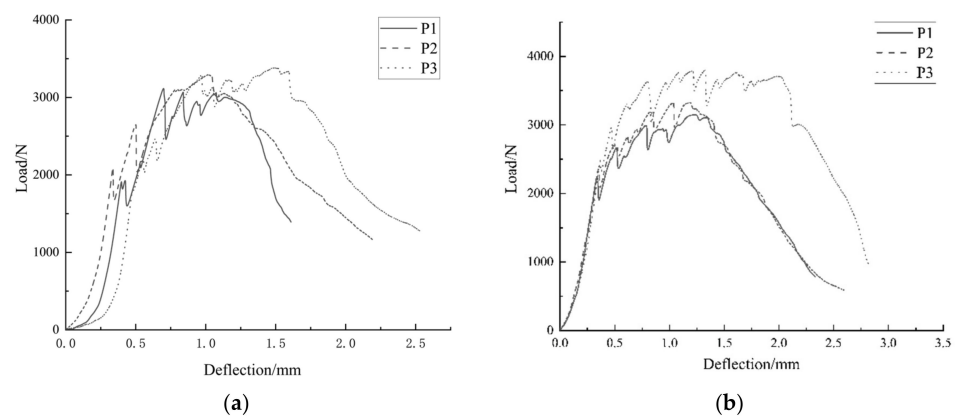


Figure 6. Load deflection curve of ECC prepared with different types of fly ash: (a) 3 days load deflection curve; (b) 28 days load deflection curve.

Table 3. Bending toughness of ECC prepared with different types of fly ash kJ/m^3 .

Date	P1	P2	P3
3 days	23	36	60
28 days	32	42	85

According to the calculation results of equivalent bending toughness, compared with the P1 and P2 groups, the bending toughness of the P3 group increased by 160.8% and 66.7% at 3 days and by 165.6% and 102.4% at 28 days, respectively. As the particle size of the fly ash decreases, the bending toughness of the mortar block increases. Combined with Figure 5c, the flexural compression ratio is $P3 > P2 > P1$. With the decrease in the fly ash particle size, the flexural compression ratio increases, which shows that the ECC made of ground fly ash composite PVA fiber has better flexural toughness. This is because the ground fly ash improves the uniformity of the PVA fiber dispersion in the matrix. When cracks appear, more evenly distributed fibers can play a better role in controlling crack propagation. At the same time, the irregularly shaped ground fly ash particles weaken the “ball effect”, and a large number of closely packed fly ash particles enhance the friction between the fiber and the matrix, improve the fiber interface bonding performance and

improve the fiber reinforcement effect so as to significantly improve the bending toughness of the mortar block.

3.3. Effect of Different Types of Fly Ash on Rheological Properties of ECC

In order to explore the influence of different types of fly ash on the dispersion effect of the PVA fiber in the concrete, we carried out experiments on the rheological properties of fly ash with different types, and we evaluated its rheological properties by studying yield stress and plastic viscosity [25]. The test was conducted to prepare slurry by removing the PVA fiber and quartz sand on the basis of the original ratio. The shear stress curve and plastic viscosity curve are shown in Figure 7.

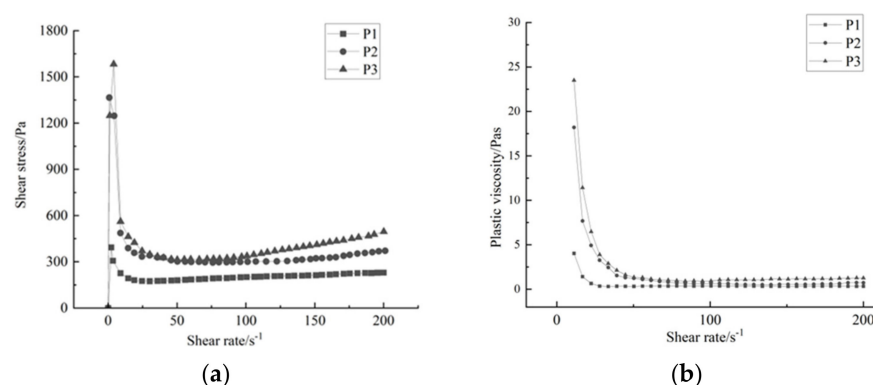


Figure 7. Rheological property curve of ECC prepared with different types of fly ash: (a) shear stress curve; (b) plastic viscosity curve.

As a viscoplastic material, fresh cement paste needs to overcome the yield stress before flow can occur, which belongs to non-Newtonian fluids [26]. According to Figure 7a, the shear rate is low and the cement slurry undergoes elastic deformation. When the shear stress reaches a certain value, the material in the slurry flows so that the maximum shear stress required for the flow of the slurry material is the static yield stress. The P1, P2 and P3 groups reached 393.11 Pa, 1248.53 Pa and 1582.37 Pa, respectively. As the shear rate increases, the particles agglomerated inside the slurry are subjected to shear stress, the agglomerated structure is destroyed [27], the agglomerated structure is dispersed as the particles flow along the direction of shear and the flow resistance decreases, corresponding to the image of the falling section after the static yield stress. When the shear rate reaches the critical value, only a low shear stress is required to maintain the flow of the cement paste. When the shear rate exceeds the critical value, the organized flow state between the particles is disturbed, the particles collide with each other to form new aggregates and the shear stress increases. When the shear rate exceeds the critical value, the shear stress increases linearly with the increase in the shear rate, showing the characteristics of a typical Bingham model curve [26]. The critical value of the shear rate of the raw fly ash is 19.08 s^{-1} . When the shear rate exceeds 19.08 s^{-1} , the shear stress increases linearly at the rate of $0.33 \text{ Pa}\cdot\text{s}$. The critical value of the shear rate of the sorted fly ash and the ground fly ash is about 50.13 s^{-1} . When the shear rate is greater than 50.13 s^{-1} , the shear rate of the sorted fly ash increases linearly at a rate of $0.6 \text{ Pa}\cdot\text{s}$, while the shear rate of the ground fly ash increases linearly at a rate of $1.12 \text{ Pa}\cdot\text{s}$.

In order to study the effect of the different particle sizes of the fly ash on the rheological properties of the slurry, two rheological parameters, yield stress τ_0 and plastic viscosity μ , were experimentally analyzed, and their rheological equations were fitted based on the Bingham model for fresh cement slurry according to the calculation formula (2). The results are shown in Table 4.

Table 4. Rheological equation of ECC prepared with different types of fly ash.

Number	Yield Stress τ_0	Plastic Viscosity μ	Rheology Equation
P1	164.0	0.33	$\tau = 0.33\gamma + 164$
P2	240.9	0.60	$\tau = 0.6\gamma + 240.9$
P3	246.9	1.21	$\tau = 1.21\gamma + 246.9$

As the ratio of the shear stress and shear rate, plastic viscosity represents the sum of the internal friction resistance of the slurry; the greater the plastic viscosity, the worse the fluidity of the slurry. The plastic viscosity of the three slurries showed a decreasing trend, and then an increasing trend with the increase in the shear rate; that is, the plastic viscosity of the slurry showed the shear–thinning phenomenon first with the increase in the shear rate. When the shear rate increases to a critical value, the plastic viscosity of the slurry gradually increases and stabilizes [28]. Combined with Table 4, the plastic viscosity of group P1 is the lowest, at only 0.33 Pa·s, that of group P2 is 0.6 Pa·s and that of group P3 is the highest, reaching 1.21 Pa·s.

According to Figure 2a, the different particle sizes and morphologies of fly ash, the raw fly ash has spherical particles with smooth surfaces, giving rise to the ball effect in cement. This is conducive to the relative sliding between slurry particles, thus showing a lower yield stress and plastic viscosity. Compared with the raw fly ash, the sorted fly ash has spherical particles, but the particle size is smaller, and the specific surface area is larger. Under conditions where the water–cement ratio remains unchanged, the free water acting as lubrication between the slurry particles decreases, and the friction between the particles increases, so as to increase the yield stress and plastic viscosity. The particle size of the ground fly ash is the smallest, and the specific surface area is the largest. Therefore, the free water content between the particles playing a role in lubrication is reduced, which increases the friction force in the slurry [29]. Moreover, the spherical particles of the ground fly ash are transformed into angular particles under the same amount of fly ash; the number of spherical particles is reduced, weakening the morphology effect. Moreover, due to the existence of angular particles, the friction force between the particles is increased, so group P3 shows the highest yield stress and plastic viscosity.

The ground fly ash shows a high yield stress and plastic viscosity. When mechanical vibration occurs, the fiber can flow only after overcoming the large internal resistance of the slurry; it is evenly dispersed in the matrix and does not easily float. Therefore, the P3 group shows a better flexural strength and bending toughness.

4. Conclusions

This study reported the outcomes of experimental and theoretical analyses on the compressive strength, flexural strength and flexural toughness of ECC prepared from fly ash with different preparation methods. The ECC was added with different types of fly ash (raw fly ash, sorted fly ash and ground fly ash). Considering different types of fly ash, the mechanical characteristics of ECC were studied by measuring the mortar compressive strength, flexural strength and bending toughness, and the rheological properties of ECC were studied by measuring the fly ash slurry rheological test. The following conclusions were drawn:

1. Compared with raw fly ash and sorted fly ash, ground fly ash has a smaller particle size and a larger specific surface area. In the early stages of ECC hydration, it can play a filling role and increase the density of the ECC matrix. Compared with ECC prepared using raw fly ash and sorted fly ash, the 3 days compressive strength of ground fly ash group ECC matrix increased by 11.4% and 5.8%, respectively. In the later stages of ECC hydration, ground fly ash can better exert the pozzolanic effect and generate more cementitious materials. Compared with ECC prepared using raw

- fly ash and sorted fly ash, the 28 days compressive strength of ground fly ash group ECC increased by 9.7% and 4.2%, respectively.
2. As the particle size of fly ash decreases with the decrease of fly ash particle size, the specific surface area increases. Under the condition of keeping the water cement ratio of ECC unchanged, the friction force between particles of the ground fly ash group ECC increases. Compared with the other two groups, the spherical particles of ground fly ash change to become irregular angular particles, which weakens their morphological effect, and increases the friction between particles in the ECC slurry. Therefore, the ground fly ash group ECC shows the maximum yield stress 246.9 Pa and plastic viscosity 1.21 Pa.s.
 3. The ground fly ash increases the yield stress and plastic viscosity of cement ECC slurry, thus improving the dispersion of PVA fiber in ECC. When the matrix is damaged by bending, failure occurs in the matrix, though the ground fly ash group ECC still maintains a good load-bearing holding capacity when reaching the peak load, showing better flexural strength and bending toughness. Compared with the raw fly ash group ECC and the sorted fly ash group ECC, the flexural strength of the ground fly ash group ECC increased by 18.92% and 10.69% in 28 days, and the bending toughness increased by 165.6% and 102.4% in 28 days, respectively.

The addition of fly ash has a certain effect on the improvement of the mechanical properties of ECC, and also plays a role in improving its durability. It can also extend the service time of ECC under complex soil conditions and extreme natural climates. The effect of different types of fly ash on the mechanical properties of ECC with longer hydration age requires further study. In addition, the influence of different types of fly ash on the durability of ECC is also an important consideration for subsequent research.

Author Contributions: Conceptualization, X.W. and J.M.; methodology, K.S.; software, K.S.; validation, X.W. and J.M.; formal analysis, X.W.; investigation, J.S.; resources, J.S.; data curation, X.W.; writing—original draft preparation, X.W. and K.S.; writing—review and editing, X.W. and K.S.; visualization, J.M. and J.S.; supervision, X.W.; project administration, J.M.; funding acquisition, J.S. All authors have read and agreed to the published version of the manuscript.

Funding: This research was funded by Henan Provincial Department of Transportation Technology Project, grant number 2020J-2-11.

Conflicts of Interest: The authors declare no conflict of interest.

References

1. Valvona, F.; Toti, J.; Gattulli, V.; Potenza, F. Effective seismic strengthening and monitoring of a masonry vault by using Glass Fiber Reinforced Cementitious Matrix with embedded Fiber Bragg Grating sensors. *Compos. Part B-Eng.* **2017**, *113*, 355–370. [[CrossRef](#)]
2. Kunieda, M.; Rokugo, K. Recent Progress on HFRCC in Japan. *J. Adv. Concr. Technol.* **2006**, *4*, 19–33. [[CrossRef](#)]
3. Marcalikova, Z.; Cajka, R.; Bilek, V.; Bujdos, D.; Sucharda, O. Determination of Mechanical Characteristics for Fiber-Reinforced Concrete with Straight and Hooked Fibers. *Crystals* **2020**, *10*, 545. [[CrossRef](#)]
4. Pujadas, P.; Blanco, A.; Cavalaro, S.H.P.; De La Fuente, A.; Aguado, A. The need to consider flexural post-cracking creep behavior of macro-synthetic fiber reinforced concrete. *Constr. Build. Mater.* **2017**, *149*, 790–800. [[CrossRef](#)]
5. Li, V.C.; Kanda, T. Innovations Forum: Engineered Cementitious Composites for Structural Applications. *J. Mater. Civ. Eng.* **1998**, *10*, 66–69. [[CrossRef](#)]
6. Curosu, I.; Liebscher, M.; Alsous, G.; Muja, E.; Li, H.; Drechsler, A.; Frenzel, R.; Synytska, A.; Mechtcherine, V. Tailoring the crack-bridging behavior of strain-hardening cement-based composites (SHCC) by chemical surface modification of poly(vinyl alcohol) (PVA) fibers. *Cem. Concr. Compos.* **2020**, *114*, 103722. [[CrossRef](#)]
7. Lepech, M.D.; Li, V.C. Application of ECC for bridge deck link slabs. *Mater Struct.* **2009**, *42*, 1185–1195. [[CrossRef](#)]
8. Haskett, M.; Mohamed Sadakkathulla, M.; Oehlers, D.; Guest, G.; Pritchard, T.; Sedav, V.; Stapleton, B. Adelaide Research and Scholarship: Deflection of GFRP and PVA fibre reinforced concrete beams. In Proceedings of the 6th International Conference on FRP Composites in Civil Engineering (CICE2012), Rome, Italy, 13–15 June 2012.
9. Li, V.C.; Wang, S.; Wu, C. Tensile strain-hardening behavior of polyvinyl alcohol engineered cementitious composite (PVA-ECC). *ACI. Mater. J.* **2001**, *98*, 483–492.

10. Hengmao, N.; Wenhong, W.; Yanru, Z. Analysis of flexural properties of cement-based materials based on PVA fiber matrix interface properties. *Mater. Guide* **2018**, *32*, 995–999.
11. Hussein, A.A.E.; Shafiq, N.; Nuruddin, M.F. Compressive strength and interfacial transition zone of sugar cane bagasse ash concrete: A comparison to the established pozzolans. *AIP Conf. Proc.* **2015**, *1660*, 070002. [[CrossRef](#)]
12. Kapoor, K.-M.-E.; Singh, S.-P.; Singh, B. Durability of self-compacting concrete made with Recycled Concrete Aggregates and mineral admixtures. *Constr. Build. Mater.* **2016**, *128*, 67–76. [[CrossRef](#)]
13. Izabela, K.; Kacper, J. Study of compressive strength evolution in soil cement samples with fly-ash admixtures. *Mater. Sci. Eng.* **2018**, *365*, 032049.
14. Liang, L.; Xu, Y.; Hu, S. Bending and Crack Evolution Behaviors of Cemented Soil Reinforced with Surface Modified PVA Fiber. *Materials* **2022**, *15*, 4799. [[CrossRef](#)]
15. Alexandra, A.E.; Jarosław, R.; Damian, S.; Przemysław, Z. Basic Aspects of Deep Soil Mixing Technology Control. *Mater. Sci. Eng.* **2017**, *245*, 022019.
16. Elena, A.E.; Alexander, L.I.; Marat, M.K.; Cheynesh, B.K.; Yulia, S.T. Creation of a Nanomodified Backfill Based on the Waste from Enrichment of Water-Soluble Ores. *Materials* **2022**, *15*, 3689.
17. Zhang, Z.; Liu, J.-C.; Xu, X.; Yuan, L. Effect of sub-elevated temperature on mechanical properties of ECC with different fly ash contents. *Constr. Build. Mater.* **2020**, *262*, 120096. [[CrossRef](#)]
18. Khatib, J.; Jahami, A.; El Kordi, A.; Sonebi, M.; Malek, Z.; Elchamaa, R.; Dakkour, S. Effect of municipal solid waste incineration bottom ash (MSWI-BA) on the structural performance of reinforced concrete (RC) beams. *J. Eng. Des. Technol.* **2021**. [[CrossRef](#)]
19. Liu, P.; Hai, R.; Liu, J.; Huang, Z. Mechanical Properties and Axial Compression Deformation Property of Steel Fiber Reinforced Self-Compacting Concrete Containing High Level Fly Ash. *Materials* **2022**, *15*, 3137. [[CrossRef](#)]
20. Ma, J.; Wang, D.; Zhao, S. Influence of Particle Morphology of Ground Fly Ash on the Fluidity and Strength of Cement Paste. *Materials* **2021**, *14*, 283. [[CrossRef](#)]
21. Chen, A.; Li, C. Strength analysis of fly ash cement prepared by grinding fly ash. *Concrete* **2020**, *1*, 64–68.
22. Lee, S.H.; Kim, H.J.; Sakai, E. Effect of particle size distribution of fly ash–cement system on the fluidity of cement pastes. *Cem. Concr. Res.* **2003**, *33*, 763–768. [[CrossRef](#)]
23. Yan, P. Action mechanism of fly ash in the hydration process of composite cementitious materials. *J. Silicic Acid.* **2007**, *51*, 172–179.
24. Wang, Q.; Wen, W. Effect of fly ash content on strain hardening properties of PVA-ECC. *J. Beijing Univ. Technol.* **2021**, *47*, 321–327.
25. Termkhajornkit, P.; Nawa, T. The fluidity of fly ash-cement paste containing naphthalene sulfonate superplasticizer. *Cem. Concr. Res.* **2004**, *34*, 1017–1024. [[CrossRef](#)]
26. Barnes, H.A.; Hutton, J.F.; Walters, K. *An Introduction to Rheology*; Elsevier: Amsterdam, The Netherlands, 1989.
27. Jiao, H.; Yachuang, W. Microscale mechanism of sealed water seepage and thickening from tailings bed in rake shearing thickener. *Miner. Eng.* **2021**, *173*, 107043. [[CrossRef](#)]
28. Laskar, A.I.; Talukdar, S. Rheological behavior of high performance concrete with mineral admixtures and their blending. *Constr. Build. Mater.* **2007**, *22*, 8–10. [[CrossRef](#)]
29. Jiao, H.; Chen, W. Flocculated unclassified tailings settling efficiency improvement by particle collision optimization in the feed-well. *Int. Miner. Metall. Mater.* **2022**. [[CrossRef](#)]